Catalytic degradation of organic pollutant by biosynthesized silver nanoparticles using Trigonella foenum-graceum L. leaves

Monika Moond
Chaudhary Charan Singh Haryana Agricultural University
Sushila Singh (singhsushila999@gmail.com)
Chaudhary Charan Singh Haryana Agricultural University
Seema Sangwan
Chaudhary Charan Singh Haryana Agricultural University
Ritu Devi
Chaudhary Charan Singh Haryana Agricultural University
Anuradha Beniwal
Chaudhary Charan Singh Haryana Agricultural University
Jyoti Rani
Chaudhary Charan Singh Haryana Agricultural University
Rajita Beniwal
Chaudhary Charan Singh Haryana Agricultural University
Rajni Kant Sharma
Chaudhary Charan Singh Haryana Agricultural University

Research Article

Keywords: green synthesis, Silver nanoparticles, optimized, morphology, catalyst

Posted Date: April 17th, 2023

DOI: https://doi.org/10.21203/rs.3.rs-2789385/v1

Abstract

The usefulness of plant extracts in the green synthesis of silver nanoparticles (AgNPs) have received a lot of interest since it is easy, environmentally benign, stable and economical. The present study involves biosynthesis of AgNPs using *Trigonella foenum-graceum* L. leaf extract belonging to specific variety HM (Hisar Mukta) 425. The different reaction conditions such as amount of leaf extract, temperature, concentration of silver nitrate, pH and incubation period were optimized by using UV-Visible spectrophotometer. The average particle size, morphology and elemental composition of the AgNPs were studied through UV-Vis spectroscopy, Particle size analyser (PSA), Field emission scanning electron microscopy (FESEM), X-ray diffraction (XRD), High resolution transmission electron microscopy (HRTEM) and Fourier Transform Infrared Spectroscopy (FTIR). The average size of AgNPs was found to be 19 nm and were spherical in shape. The efficacy of AgNPs as a catalyst was confirmed by the 13 minutes completion of the organic pollutant p-nitrophenol (p-NP) reduction. Their catalytic capabilities strongly support the use of AgNPs in the purification of contaminated water.

1 Introduction

Noble metal nanostructures have drawn a lot of attention recently as a result of the development of nanotechnology and its potential to make significant contributions to the disciplines of renewable energy, plasmonic, catalysis, and photocatalysis [1–3]. As a result, the technology for developing them have been improved to produce shape, size, and geometry-controlled nanostructures to support various applications. Metal nanoparticles have attracted a lot of attention in both research and industrial applications. AgNPs have drawn a lot of interest among them because of their distinct optical, electronic, and catalytic features [4, 5].

A variety of physical and chemical processes can be used to create AgNPs, but doing so may have unintended environmental effects due to high energy consumption, the release of toxic and dangerous chemicals, the use of complicated equipment, and the synthesis conditions. It is always preferable to use green chemistry as an alternative to conventional methods due to the growing awareness of the detrimental effects that synthetic methods have on the environment. As a result, many biological agents such as plants, bacteria, fungi and algae have been reported to synthesize AgNPs on their own without the need for additional stabilising and reducing agents. The method using plants to synthesize AgNPs is preferable to the one using microbes since it is less hazardous to living organisms, versatile and does not require maintenance of cell culture [6, 7]. Among the diverse bio-reductants, *Trigonella foenum-graceum* L. leaves were chosen in the present study. It is an annual herb also known as Methika (Sanskrit), Greek hay, Fenugreek (English), Kasuri methi, Sag methi (Hindi) and Methi (Marathi) which belongs to family Fabaceae. Due to the existence of numerous bioactive compounds such as apigenin, orientin, luteolin, vitexin quercetin, isovitexin, amino acids, saponins, alkaloids and phenols, it is used to cure a variety of diseases. These phytochemicals can be utilized as reducing and capping agents to synthesize biogenic nanoparticles [8, 9].

AgNPs are now frequently employed to enhance the catalytic efficiency of reduction processes. They are employed in the one-step reduction of organic pollutant nitroaromatics to produce amino aromatics. The synthesis of amino aromatics from nitroaromatics is very interesting since amino aromatics are crucial building blocks for the synthesis of herbicides, dyes, antioxidants, medicines, polymers and other fine chemicals [10, 11]. The catalytic hydrogenation of nitroaromatics employing iron, tin, zinc, Au/SiO_2, Au/Al_2O_3, Pd/TiO_2, Pt-Ne bimetallic nanoparticles and Pt/TiO_2 can easily produce amino aromatics [12]. All of these processes have drawbacks, such as the need for hazardous solvents, potent reducing agents, expensive metals like Pt, Au and Pd, heat, high pressure and the production of hazardous byproducts. However, using AgNPs to reduce nitroaromatics is far superior to using any of these other methods because it is less expensive, non-toxic, produces no dangerous byproducts, and only needs ambient temperature and pressure [13]. The toxic and persistent organic pollutant known as p-nitrophenol has caused widespread concern because of its negative effects, particularly on human health. It causes contamination of surface as well as groundwater. Water becomes contaminated as a result (surface and groundwater). Conversion of p-nitrophenol to p-aminophenol has become a crucial issue because p-aminophenol (p-AP) is a compound with a lower degree of toxicity [14].

In this current study, we synthesized Silver nanoparticles (AgNPs) using *Trigonella foenum-graceum* L. leaf extract by optimizing reaction conditions like amount of extract, concentration of Silver nitrate, temperature, pH of reaction medium and incubation time. Then, fabricated nanoparticles were characterized by using UV-Vis spectroscopy, Field emission scanning electron microscopy (FESEM), Particle size analyser (PSA), X-ray diffraction (XRD), High resolution transmission electron microscopy (HRTEM) and Fourier Transform Infrared Spectroscopy (FTIR).The catalytic activity of AgNPs for reduction of organic pollutant p-nitrophenol to p-aminophenol has been studied.

2 Materials And Methods

2.1 Chemicals and collection of plant material

Himedia Private Limited supplied the silver nitrate ($AgNO_3$), sodium borohydride ($NaBH_4$) and p-nitrophenol.

Trigonella foenum-graecum L. variety Hisar Mukta (HM) 425 leaves were acquired from the Vegetable Science Research Farm at Chaudhary Charan Singh Haryana Agricultural University. The obtained sample was examined using a website by the botany and plant physiology department at CCS HAU in Hisar, India (Tropicos & IPNI). Utilizing voucher specimen number 20, the department of genetics and plant breeding at CCS HAU Hisar evaluated the validity of the voucher specimens for medicinal, aromatic, and potential crops.

2.2 Preparation of aqueous leaves extract

50 mL of deionized water and 5 grams of powdered dried leaves were heated at 60°C for 30 minutes. The leaves extract was centrifuged for 15 minutes at 7500 rpm after filtering with Whatman Filter Paper No. 1

and then stored at 4°C for further research.

2.3 Synthesis of Silver nanoparticles (AgNPs) using aqueous leaves extract

For the synthesis of silver nanoparticles, the reaction parameters including the quantity of extract, the temperature, the concentration of $AgNO_3$, the pH of the reaction medium, and the incubation time were optimised (AgNPs). Then, synthesis was performed under ideal circumstances: 0.2 mL of aqueous leaves extract was added to 25 mL of $AgNO_3$. The reaction mixture was stirred for 60 minutes at 45^0C degrees Celsius. Instantaneously, the reaction mixture's light yellow colour turned dark brown. The reduction reaction took place after the reaction mixture was incubated for 24 hours. After that, no additional colour change was noticed. The reaction mixture was centrifuged for 15 min at 15,000 rpm to precipitate AgNPs. These AgNPs were then dried in an oven and utilized for further experiments.

2.4 Characterization of Silver nanoparticles (AgNPs)

By using UV-Vis spectrophotometer (Model UV 1900, Shimadzu), the surface plasmon resonance band (SPR) of synthesized AgNPs was confirmed. Using Particle Size Analyzer (Microtracnanotrac wave II) equipment, polydispersity index (PDI) and the hydrodynamic diameter of nanoparticles were determined. In order to analyse the surface morphology and elemental composition of AgNPs, a field emission scanning electron microscope (FESEM, JSM-7610FPlus) with an energy dispersive X-ray spectroscopy (EDX) detector was utilised. The crystallinity, phase composition, and purity of nanoparticles were evaluated using X-ray diffraction (XRD) on a Miniflex II desktop X-ray diffractometer with Ni-filtered filtered Cu Kα radiation (λ = 1.5418 A^0) in the 2θ range of $10–80^0$ at a scanning rate of 0.02^0 per second. High Resolution Transmission Electron Microscopy (JEM/2100 PLUS operating at 200 kV) was used to examine the morphology and selected area electron diffraction (SAED) pattern of nanoparticles. The FTIR spectrophotometer (Perkin Elmer) was used to obtain the FTIR spectra (4000 – 650 cm^{-1}).

2.5 Catalytic reduction of p-nitrophenol to p-aminophenol

To evaluate the catalytic activity of biosynthesized AgNPs, 0.01M aqueous solution of p-NP and 0.1 M solution of $NaBH_4$ were prepared. The absorbance of 40 µL of aqueous solution p-NP (0.01M) was determined using a UV-Vis spectrophotometer after being diluted up to 3mL. A freshly made 0.2 mL of $NaBH_4$ (0.1M) aqueous solution was mixed with an aliquot of 40 µL of p-NP solution (0.01M), which was then diluted with deionized water to make a volume of 3 mL. The absorbance of this mixture was then determined. Lastly, 30 µL of AgNPs were added to the aforementioned reaction mixture and vigorously shaken. UV-Vis spectrophotometer measured the progress of the reaction. The concentration of sodium borohydride could be thought of as constant throughout the reaction because it was greater than the concentration of p-NP. The concentration of p-NP had an impact on the reaction rate, and as a result, the reaction followed pseudo first-order kinetics. A plot of ln (A/A^0) as a function of time was created to study the reaction's kinetics, and the rate constant's value was determined [15].

$$\ln C/Co = \ln A/Ao$$

where, C_0 is the initial concentration, C is the concentration at time t, similarly A_0 is initial absorbance and A is absorbance at time t.

3 Results And Discussion

3.1 Optimization of biosynthesis of AgNPs Using UV-Vis Spectroscopy Analysis

3.1.1 Effect of leaves extract amount

Biosynthesis of AgNPs was performed by varying amount of leaves extract (0.1mL, 0.2mL, 0.3mL, 0.4mL and 0.5 mL) in 25 mL of 1mM $AgNO_3$ solution at room temperature and neutral pH. With increase in the ratio of leaf extract to $AgNO_3$ solution (after 0.2mL) Surface Plasmon Resonance (SPR) band got broader (Fig. 1). This can be explained by the fact that there were a lot of reductants present in the reaction medium, which sped up the reduction of Ag + ions. By a process known as Ostwald ripening, which results in an increase in nanoparticle size, the quick reduction of Ag + ions typically facilitated further growth of nanoparticles. At concentration ratio $AgNO_3$: leaves extract 25:0.2 (mL: mL) a sharp band at λ_{max} 448 nm was observed. On increasing the concentration beyond 0.5 mL, it was found that within two hours, the color of the solution turned blackish grey and the formation of AgNPs was restricted. On the basis of above observation, 0.2mL was found as the appropriate amount for the synthesis of AgNPs.

3.1.2 Effect of Silver nitrate concentration

Biosynthesis of AgNPs by using leaves extract was performed by varying $AgNO_3$ (25 mL) concentrations (0.5, 1.0, 2.0, 3.0 and 5.0 mM) with 0.2mL leaves aqueous extract at room temperature and neutral pH. From the UV-Vis data, it can be concluded that there was no synthesis of AgNPs at 0.5 mM concentration of $AgNO_3$. An intense, sharp and characteristic SPR band was observed for 1 mM $AgNO_3$ solution. The SPR band broadens and shifts slightly towards longer wavelengths (red shift) after 1 mM, indicating an increase in the size of bio-synthesised AgNPs. This increase in size may be caused by the secondary reduction process of silver ions that were adsorbed on the surface of the built nuclei at higher Ag^+ concentrations, resulting in the generation of larger nanoparticles (Fig. 2). Beyond 1mM, it was observed that agglomeration of particles started within 1 hour of synthesis probably due to insufficient amount of capping agent present in plant extract to stabilize the biosynthesized AgNPs. At 5 mM agglomeration can be clearly noticed. Therefore, 1mM concentration of $AgNO_3$ was chosen for the synthesis of AgNPs.

3.1.3 Effect of Temperature

Biosynthesis of AgNPs by using leaves extract was performed by varying temperatures (room temperature, 45ºC 60ºC, 70ºC and 80ºC) with 0.2 mL leaves extract in 25 mL of 1 mM $AgNO_3$ solution at

neutral pH for 60 minutes. Intensity of the absorption peak increased with increase in temperature. Time required for the biosynthesis of AgNPs decreased with increase of the temperature because of increase in kinetic energy of the reaction mixture. At 45°C a blue shift can be noticed, indicating the smaller size of synthesized AgNPs. Further temperature rise was accompanied by an increase in peak broadness and a decrease in SPR intensity, indicating that the leaves extract's reducing and stabilising properties decreased at higher temperatures (Fig. 3). Keeping in view, that the stability of plant metabolites present in reaction mixture requires working at ambient temperature, therefore 45°C was chosen as the optimum temperature for the synthesis of AgNPs.

3.1.4 Effect of pH

Biosynthesis of AgNPs by using leaves extract was performed by varying pH (3, 5, 7, 9 and 11) with 0.2 mL extract in 25 mL of 1 mM silver nitrate at room temperature. The initial pH of $AgNO_3$ solution played important role during synthesis of AgNPs. From UV-Vis spectra (Fig. 4), it can be revealed that with increase in pH of metal salt solution, intensity of SPR band increased. This shift of absorbance maxima clearly indicated that the size of AgNPs decreased when pH of solution was changed from 3 to 7 (acidic to neutral). Further increase in pH from 7 to 11 (neutral to basic), agglomeration was noticed after 2 hours. The optimum pH for nanoparticles synthesis was chosen to be pH 7.

3.1.5 Effect of incubation time

At room temperature, 0.2 mL extract in 25 mL of 1 mM silver nitrate at neutral pH and varying reaction duration from 1 hour to 24 hours was used for the biosynthesis of AgNPs. UV-Vis spectra of reaction media at different time intervals (1 hour to 24 hours) were shown in Fig. 5. From the spectra, it can be observed that not significant or very low reduction of the reaction media occurred in first 1 hour of the reaction. Intensity of SPR band increased with the passage of time and became almost constant after 24 hours of incubation. Intense reddish brown colour was observed at the end of the reaction. A plot of maximum absorbance versus time revealed that there was increase in absorption during 1 hour to 24 hours, but thereafter there was no significant change in maximum absorbance was noted, which indicated that reduction has been completed. Optimized reaction conditions for biosynthesis of AgNPs by using aqueous leaves extract were mentioned in Table 1.

Table 1
Optimized reaction conditions for biosynthesis of AgNPs by using aqueous leaves extract

Optimization of reaction conditions	Corresponding values
Condition	Dark
Temperature	45°C
pH of the medium	7
Fenugreek seed extract amount	0.2mL
$AgNO_3$ concentration	1mM
Incubation time	24 hours

3.2 Characterization of biosynthesized AgNPs

3.2.1 UV-Visible Spectroscopy

Using a UV-Visible spectrophotometer, the chemical reaction between the dissolved silver ions and leaf extract was investigated. AgNPs were formed after the reaction was completed. Because of the surface plasmon resonance phenomenon 16], UV-visible analysis revealed an absorption peak at 450 nm shown in Fig. 6.

3.2.2 Particle Size Analyzer

The PSA size distribution of AgNPs was shown in Fig. 7. The polydispersity index (PDI) and hydrodynamic diameter of AgNPs was 0.2615 and 60.15 nm respectively. PSA measured the hydrodynamic diameter of synthesized AgNPs in reaction mixture which includes the whole thickness of layer of capping or reducing agents adsorbed on the surface of nanoparticles [17].

3.2.3 FESEM analysis

FESEM analysis was used to investigate the surface morphology and chemical composition of the biosynthesized AgNPs. Biosynthesized AgNPs were found to be mostly spherical with an average size 19nm (Fig. 8). The coexistence of small and large sized nanoparticles was caused by their time variation in formation during synthesis, which revealed that new nanoparticle formation and aggregation occurred simultaneously. Energy disperse X-ray (EDX) spectroscopy was performed to determine the elemental composition of the nanoparticles (Table 2).

The EDX analysis of AgNPs possesses metallic Silver (19.71%) along with other elements Carbon (19.99%), Oxygen (59.40) and Chlorine (0.90%)

Table 2 EDX analysis parameters of AgNPs

Element	Weight %	Atomic %
Carbon	19.99	29.80
Oxygen	59.40	66.48
Silver	19.71	3.27
Chlorine	0.90	0.45

3.2.4 XRD

The XRD diffraction pattern of AgNPs showed a sharp peak at 2θ (38.18º, 44.84º, 64.68º and 77.65º) corresponding to (111), (200), (220) and (311) Bragg reflections, respectively (Fig. 9). These reflections were similar to those reported for the FCC lattice structure of standard Silver (Ag) metal and are consistent with the standard data file ICSD No. 98-004-4387. The high intensity peak at 38.18º indicated a high level of crystallinity and that the (111) plane is the predominant orientation. The bio-organic phase on the particle surface is what causes the undesirable peaks between 25º and 35º [18].

3.2.5 HRTEM

By using HRTEM analysis, the morphology and size of green synthesised AgNPs were evaluated. Images of HR-TEM showing the presence of AgNPs recorded at 20nm and 50nm magnification levels in Fig. 10a and 10b respectively. The selected area electron diffraction (SAED) pattern of the synthesised AgNPs with bright spots illustrated in Fig. 10c, indicates that they are polycrystalline. The synthesized AgNPs had a spherical shape with a size range of 10 to 26 nm, with an average size of 19 nm (Fig. 10d). Their diffraction rings have been assigned the indexes 111, 200, 220, and 311, which correspond to the face cantered cubic (FCC) crystalline structure of metallic silver.

3.2.6 FTIR

FTIR analysis was performed to identify various functional groups in the leaves extract and on the surface of their biosynthesized AgNPs that were primarily responsible for the reduction of Silver nitrate (Ag^+ to Ag) and the stabilisation of AgNPs. Figure 11 depicts the FT-IR spectra of seed extract and biosynthesized AgNPs. Analysis of the FT-IR spectra of leaves revealed the presence of various characteristics peaks at 3321, 2947, 2835, 1653, 1448, 1113 and 1010 cm^{-1} and their biosynthesized AgNPs also showed peaks at 3337, 2924, 1645, 1432 and 1011 cm^{-1}, respectively (Table 3). The similarity between these two spectra with some marginal shift in peak positions confirmed that AgNPs were capped with various phytochemicals of leaf extract [19].

Table 3
Assignment of various peaks observed during FT-IR analysis

Entity	Observed Wavenumber (cm^{-1})	Assignment of peaks	Range
1	3321, 3337	O-H stretch, N-H stretch, intermolecular H-bonding	3200–3500
2	2924, 2947, 2835	C-H stretch	2700–2950
3	1645, 1653	-C = O stretch	1650–1850
4	1448, 1432	stretching vibration of alkenes C C in aromatic rings	1380–1465
5	1010,1011	C-O stretch, C-N stretch	1015–1250

3.3 Evaluation of catalytic activity

The reduction of organic pollutant p-nitrophenol to p-aminophenol by using aqueous $NaBH_4$ is a thermodynamically favourable reaction (E_0 for p-nitrophenol/p-aminophenol − 0.76 V and for H_3BO_3/BH_4 -1.33 V) but kinetically unfavourable because of large potential difference between donor and acceptor species [20]. By reacting aqueous solution of p-NP (0.01M) with a freshly prepared aqueous solution of $NaBH_4$ (0.1 M), redshift from 319.4 nm to 402 nm was observed due to the formation of 4 nitrophenolate ion (Fig. 12). Moreover, by adding 30 µL colloidal AgNPs to the reaction mixture, rapid lowering of the absorption peak at 402 nm was observed with synchronal formation of a new peak at 300 nm, thus indicating the formation of p-aminophenol. Complete disappearance of 402 nm peak was found within 13 minutes, thus indicating the completion of the reduction reaction by showing catalytic activity of biosynthesized AgNPs. Pseudo first-order rate kinetics can be applied to the reduction reaction as the concentration of the BH_4^- was much higher than p-NP [21]. The reaction rate constant (k) was found to be 0.1398 min^{-1}.

Using the probable reaction mechanism shown in Fig. 13, the catalytic reduction of p-NP by $NaBH_4$ and metal catalysts was explored. When $NaBH_4$ is ionised in the liquid phase, borohydride ions (BH_4^-) are produced, and these ions bind to the metal catalyst's surface to Using the probable reaction mechanism shown in Fig. 13, the catalytic reduction of p-NP by

Using the probable reaction mechanism shown in Fig. 13, the catalytic reduction of p-NP by $NaBH_4$ and metal catalysts was explored. When $NaBH_4$ is ionised in the liquid phase, borohydride ions (BH_4^-) are produced, and these ions bind to the metal catalyst's surface to form a metal hydride complex. p-nitrophenol simultaneously adheres to the surface of the metal hydride complex. The synthesis of the p-nitrophenolate ion (p-NP) is facilitated by the transfer of H_2 from the hydride complex surface to p-NP due

to thermodynamic equilibrium on the hydride complex surface [22]. AgNPs initiated efficient transfer of electron from donar BH_4^- ion to acceptor p-nitrophenolate ion, thereby reducing the activation energy of the reaction [23].

4 Conclusion

Silver nanoparticles were synthesized by using aqueous *Trigonella foenum-graecum L*. leaf extract which acts as both reducing agent and capping agent. The various reaction conditions like amount of leaf extract, concentration of $AgNO_3$, pH of reaction medium, temperature and incubation time were optimized for synthesis of AgNPs. The spectroscopic practices, including FESEM, UV-Visible Spectroscopy, XRD, HRTEM, and FTIR Spectroscopy were used for characterization of AgNPs. These AgNPs were additionally employed as a catalyst in the conversion of p-nitrophenol to p-aminophenol. The catalytic degradability of organic pollutant p-nitrophenol in wastewater treatment has received a lot of attention because it is one of the anthropogenic contaminants that might have a harmful impact on aquatic species.

Declarations

Acknowledgments

Monika Moond would like to thank Chaudhary Charan Singh Haryana Agricultural University, Hisar 125004, Haryana, India for providing the research facilities.

Ethical Approval

Research Involving Humans and Animals Statement not applicable

Informed Consent not applicable

Competing interests

The authors declare that they have no conflict of interest.

Authors' contributions

Participated in research design, M.M., S.S., J.R., and A.B.; Conducted experiments, M.M.; Performed data analysis, M.M. and S.S.; Wrote the manuscript, M.M.; manuscript review, S.S., R.D., R.B., S. Sangwan and R.K.S. All authors have read and agreed to the published version of the manuscript.

Funding

This research received no external funding.

Availability of data and materials not applicable

References

1. Chen, T., Pourmand, M., Feizpour, A., Cushman, B. & Reinhard, B.M. (2013). Tailoring plasmon coupling in self-assembled one-dimensional Au nanoparticle chains through simultaneous control of size and gap separation. *The journal of physical chemistry letters*, *4*(13),2147-2152.
2. Singh, S.; Sangwan, S.; Sharma, P.; Devi, P.; & Moond, M. (2021). Nanotechnology for sustainable agriculture: an emerging perspective. *Journal of Nanoscience and Nanotechnology*, *21*, 3453-3465.
3. Bogireddy, N.K.R., Pal, U., Gomez, L.M. & Agarwal, V. (2018). Size controlled green synthesis of gold nanoparticles using Coffea arabica seed extract and their catalytic performance in 4-nitrophenol reduction. *RSC advances*, *8*(44), 24819-24826.
4. Singh, J., Mehta, A., Rawat, M., Basu, S. (2018). Green synthesis of silver nanoparticles using sun dried tulsi leaves and its catalytic application for 4-Nitrophenol reduction. *Journal of Environmental Chemical Engineering*, *6*, 1468–1474.
5. Moond, M., Singh, S., Sangwan, S., Rani, S., Beniwal, A., Rani, J., Kumari, A., Rani, I. & Devi, P. (2023). Phytofabrication of Silver Nanoparticles Using Trigonella foenum-graceum L. Leaf and Evaluation of Its Antimicrobial and Antioxidant Activities. *International Journal of Molecular Sciences*, *24*(4), 3480.
6. Lee, S.H. & Jun, B.H (2019). Silver nanoparticles: synthesis and application for nanomedicine. *International journal of molecular sciences*, 20, 865.
7. Moond, M.; Singh, S.; Sangwan, S.; Devi, R.; & Beniwal, R (2022). Green Synthesis and Applications of Silver Nanoparticles*: A Systematic Review*. *AATCC Journal of Research*, *9*, 272-285
8. Dalal, R.; Singh, S.; Sangwan, S.; Moond, M. & Beniwal, R (2022). Biochemical and Molecular Mechanism of Plant-mediated Synthesis of Silver Nanoparticles–A Review. *Mini-Reviews in Organic Chemistry*, *19*, 939-954.
9. Moond, M., Singh, S., Devi, R., Beniwal, R., Matoria, P., Kumari, S., & Sharma, R.K. (2023). Proximate and mineral analysis of *Trigonella foenum-graecum* L. (Fenugreek) seeds and leaves of variety HM444. *Annals of Phytomedicine*, *12*(1),1-7.
10. Mejía, Y.R. & Bogireddy, N.K.R. (2022). Reduction of 4-nitrophenol using green-fabricated metal nanoparticles. *RSC advances*, *12*(29), 18661-18675.
11. Singh, J., Mehta, A., Rawat, M. & Basu, S. (2018). Green synthesis of silver nanoparticles using sun dried tulsi leaves and its catalytic application for 4-Nitrophenol reduction. *Journal of environmental chemical engineering*, *6*(1), 1468-1474.
12. Marcelo, G., Muñoz-Bonilla, A. & Fernández-García, M. (2012). Magnetite–polypeptide hybrid materials decorated with gold nanoparticles: study of their catalytic activity in 4-nitrophenol reduction. *The Journal of Physical Chemistry C*, *116*(46),24717-24725.
13. Deka, P., Bhattacharjee, D., Sarmah, P., Deka, R.C. & Bharali, P. (2017). Catalytic reduction of water contaminant ‘4-nitrophenol’over manganese oxide supported Ni nanoparticles. *Trends in Asian water environmental science and technology*, 35-48.

14. Achamo, T. & Yadav, O.P. (2016). Removal of 4-Nitrophenol from Water Using Ag-NP-Tridoped TiO2 by Photocatalytic Oxidation Technique Ubertas Academica. *AnAlyticAl chemistry insights*, *11*, ACI-S31508.
15. Chen, X., Zhao, D., An, Y., Zhang, Y., Cheng, J., Wang, B., & Shi, L. (2008). Formation and catalytic activity of spherical composites with surfaces coated with gold nanoparticles. *Journal of Colloid and Interface Science*, *322*(2), 414-420.
16. Bahuguna, G., Kumar, A., Mishra, N.K., Kumar, C., Bahlwal, A., Chaudhary, P. & Singh, R. (2016). Green synthesis and characterization of silver nanoparticles using aqueous petal extract of the medicinal plant Combretum indicum. *Materials Research Express*, *3*(7), 075003.
17. Kumar, B., Angulo, Y., Smita, K., Cumbal, L. & Debut, A. (2016). Capuli cherry-mediated green synthesis of silver nanoparticles under white solar and blue LED light. *Particuology*, *24*, 123-128.
18. Umadevi, M., Bindhu, M.R. & Sathe, V. (2013). A novel synthesis of malic acid capped silver nanoparticles using Solanum lycopersicums fruit extract. *Journal of Materials Science & Technology*, *29*(4), 317-322.
19. Moond, M., Singh, S., Sangwan, S., Devi, P., Beniwal, A., Rani, J., Kumari, A. & Rani, S. (2023). Biosynthesis of Silver Nanoparticles Utilizing Leaf Extract of *Trigonella foenum-graecum* L. for Catalytic Dyes Degradation and Colorimetric Sensing of Fe^{3+}/Hg^{2+}. *Molecules*, *28*, 951
20. Kong, X., Zhu, H., Chen, C., Huang, G. & Chen, Q. (2017). Insights into the reduction of 4-nitrophenol to 4-aminophenol on catalysts. *Chem. Phys. Lett.*, *684*, 148–152.
21. Kästner, C. & Thünemann, A.F. (2016). Catalytic Reduction of 4-Nitrophenol Using Silver Nanoparticles with Adjustable Activity. *Langmuir*, *32*, 7383–7391.
22. Sen, I.K., Maity, K. & Islam, S.S. (2013). Green synthesis of gold nanoparticles using a glucan of an edible mushroom and study of catalytic activity. *Carbohydrate polymers*, *91*(2), 518-528.
23. Pei, X., Qu, Y., Shen, W., Li, H., Zhang, X., Li, S., Zhang, Z. & Li, X. (2017). Green synthesis of gold nanoparticles using fungus Mariannaea sp. HJ and their catalysis in reduction of 4-nitrophenol. *Environmental Science and Pollution Research*, *24*, 21649-21659.

Figures

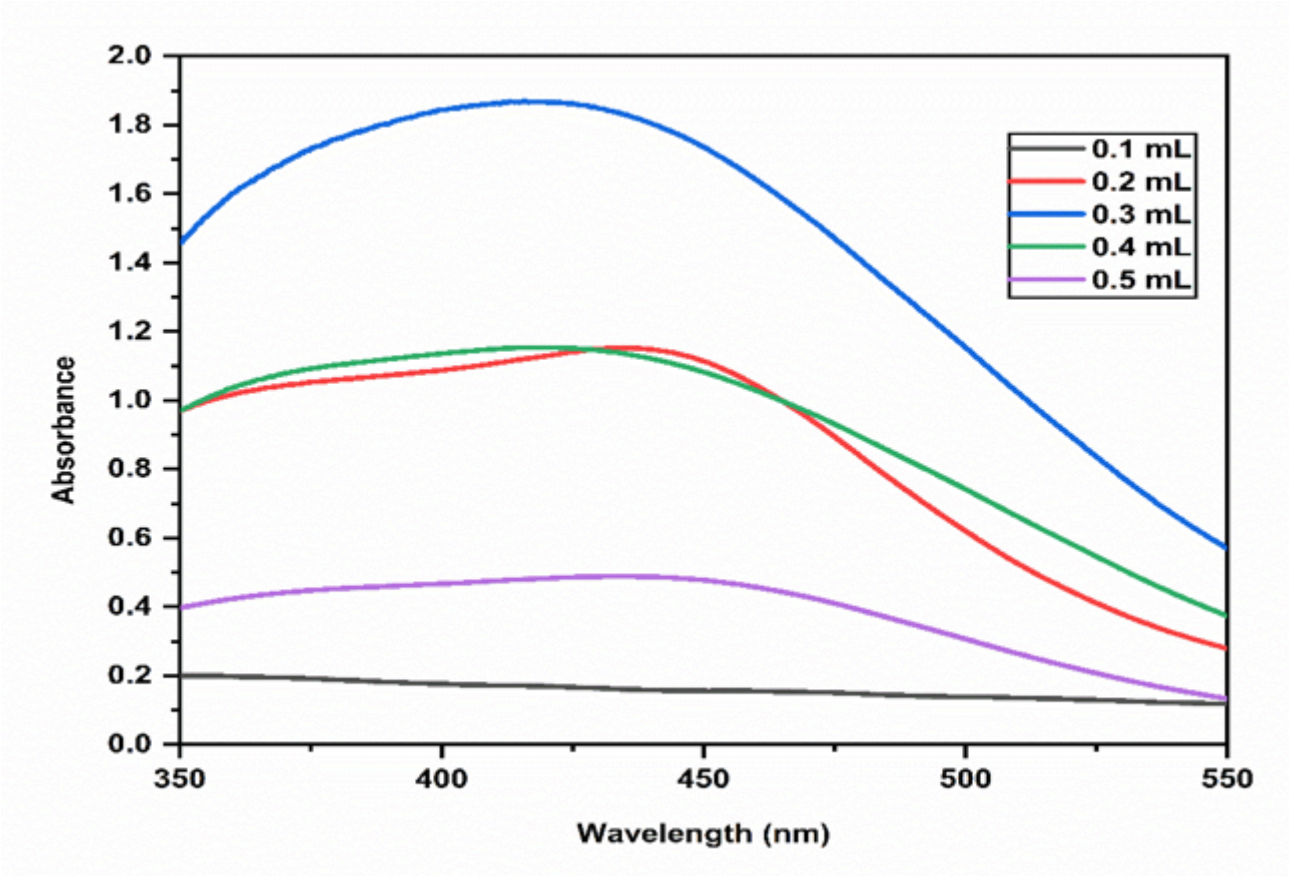

Figure 1

UV-Vis spectra showing effect of varying amount of extract on biosynthesis of AgNPs

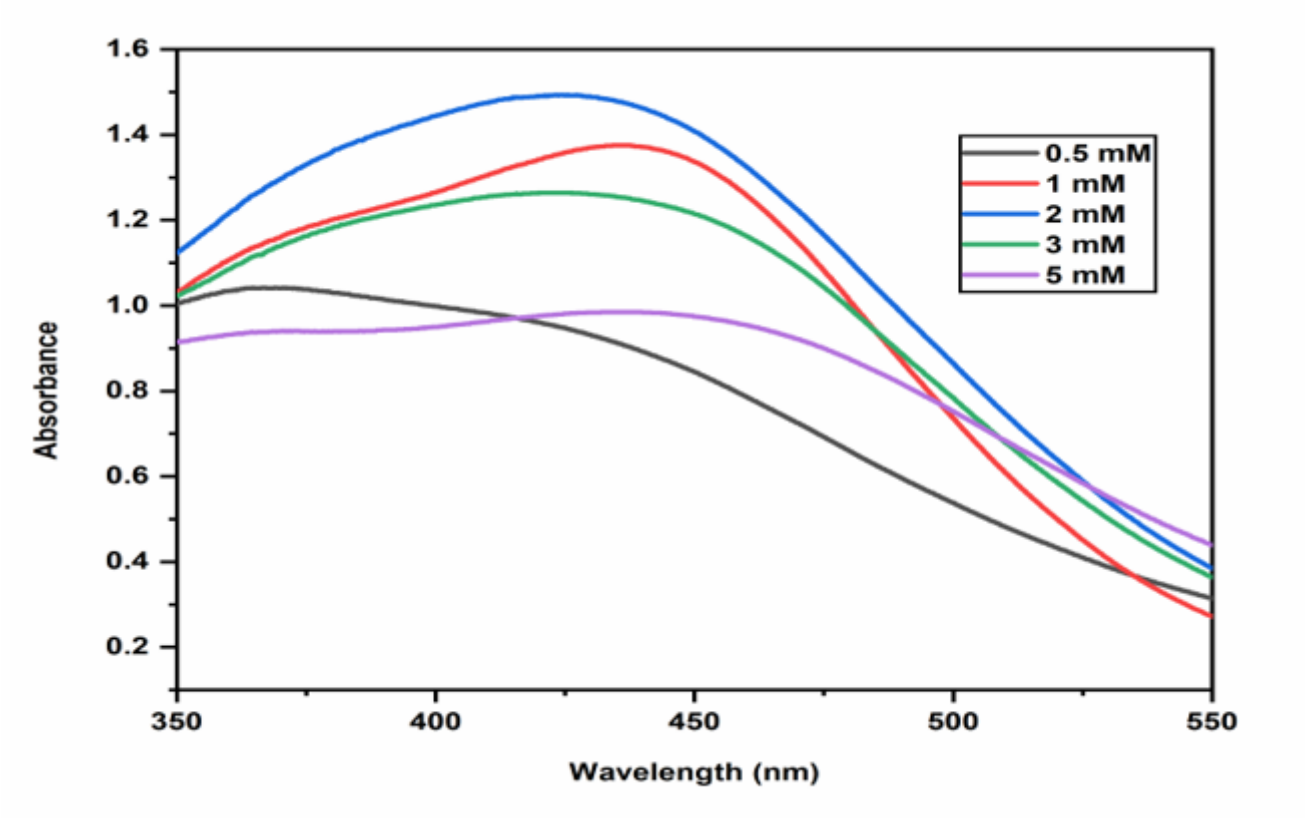

Figure 2

UV-Vis spectra showing effect of varying concentration of $AgNO_3$ on biosynthesis of AgNPs

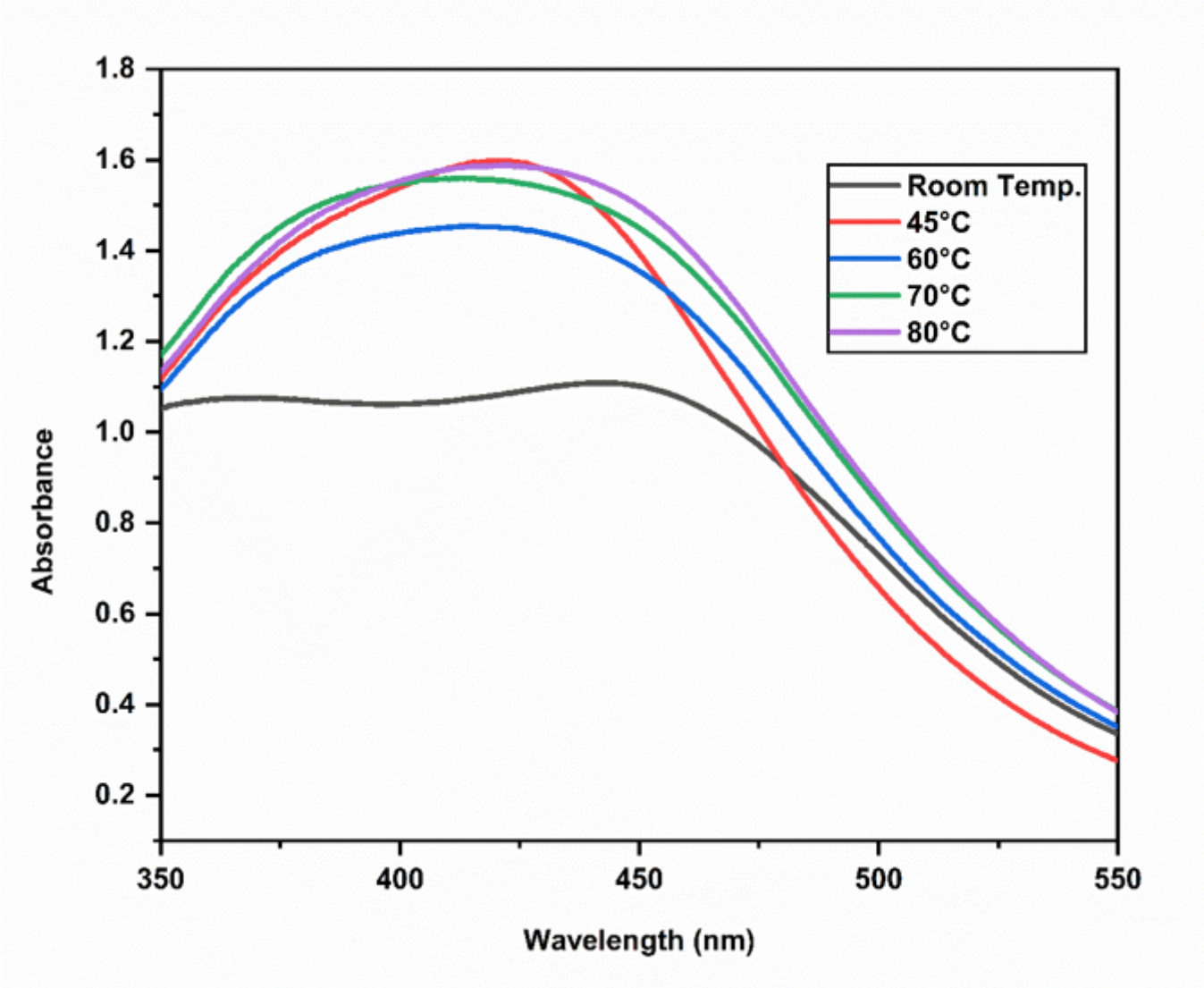

Figure 3

UV-Vis spectra showing effect of reaction temperature on biosynthesis of AgNPs

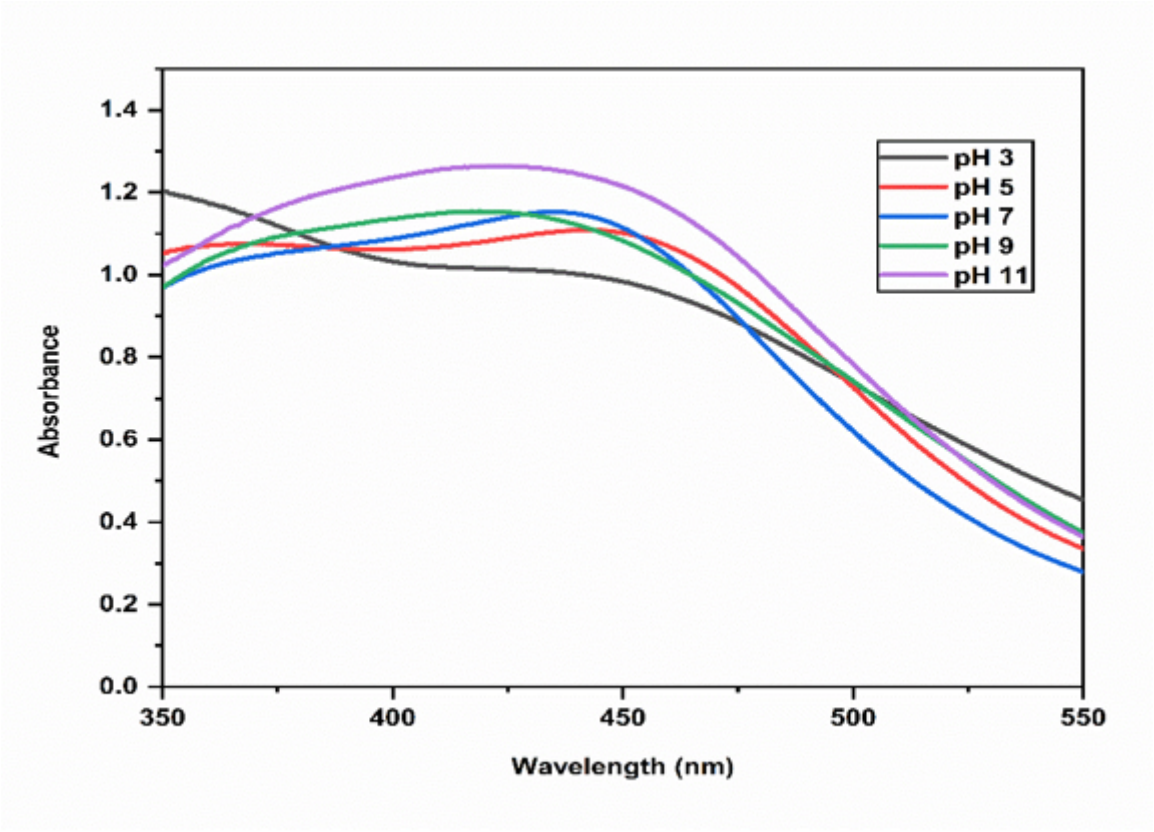

Figure 4

UV-Vis spectra showing effect of pH on biosynthesis of AgNPs

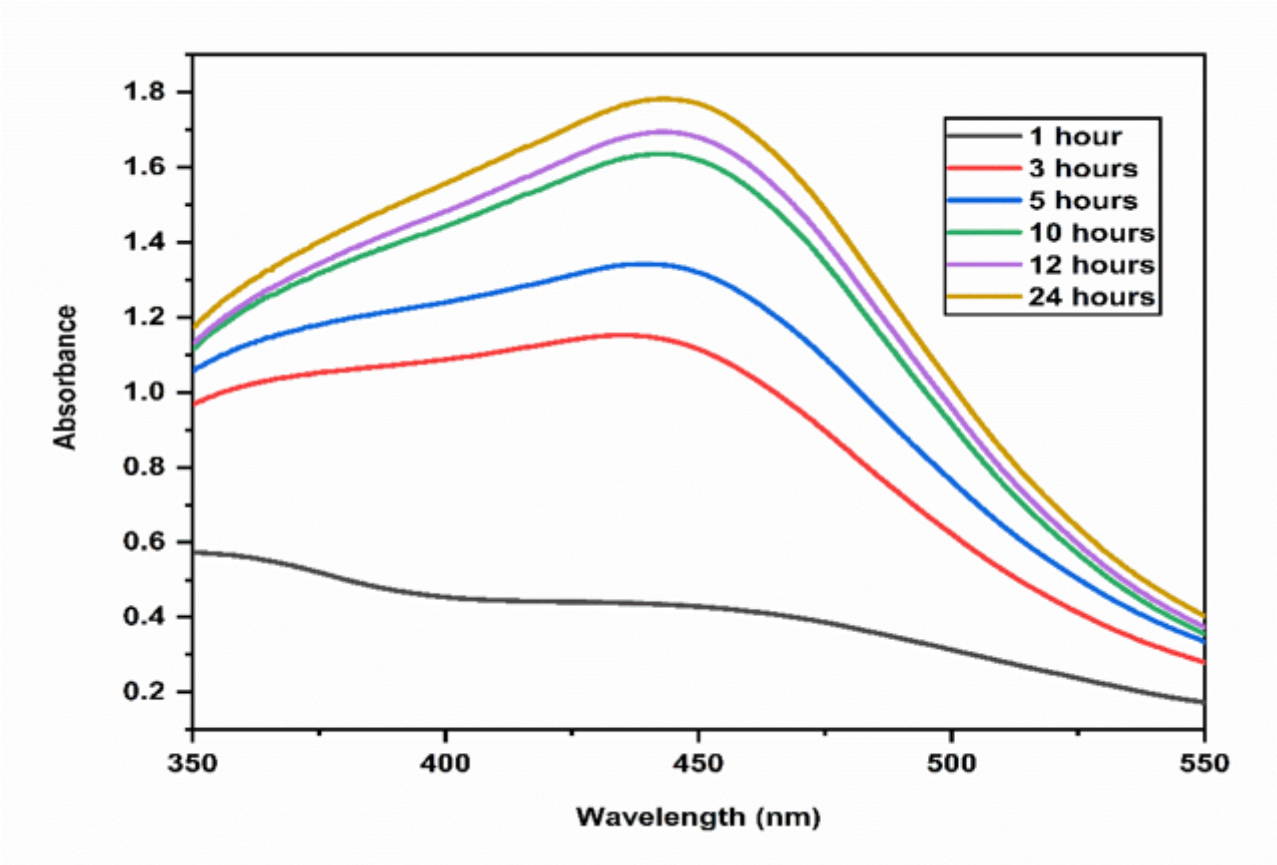

Figure 5

UV-Vis spectra showing effect of incubation time on biosynthesis of AgNPs

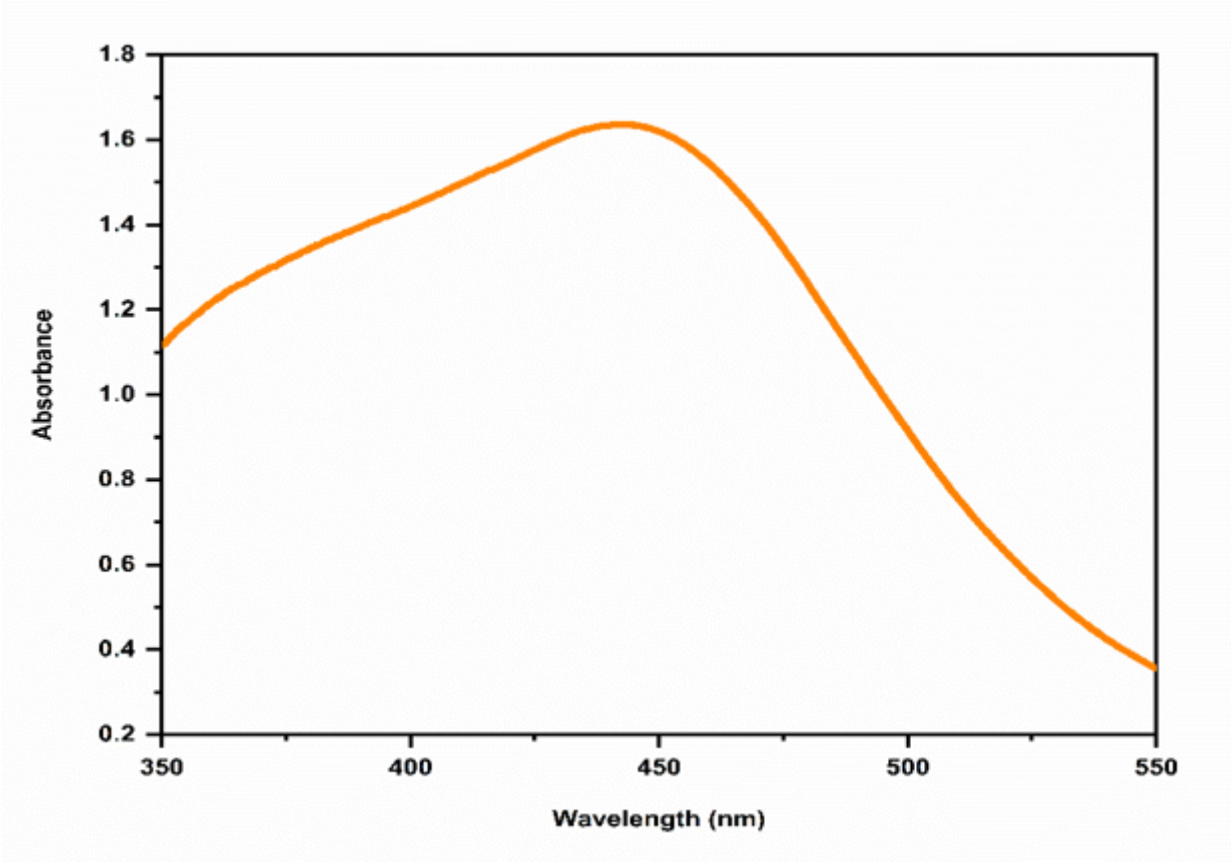

Figure 6

UV-Vis absorption spectra of AgNPs

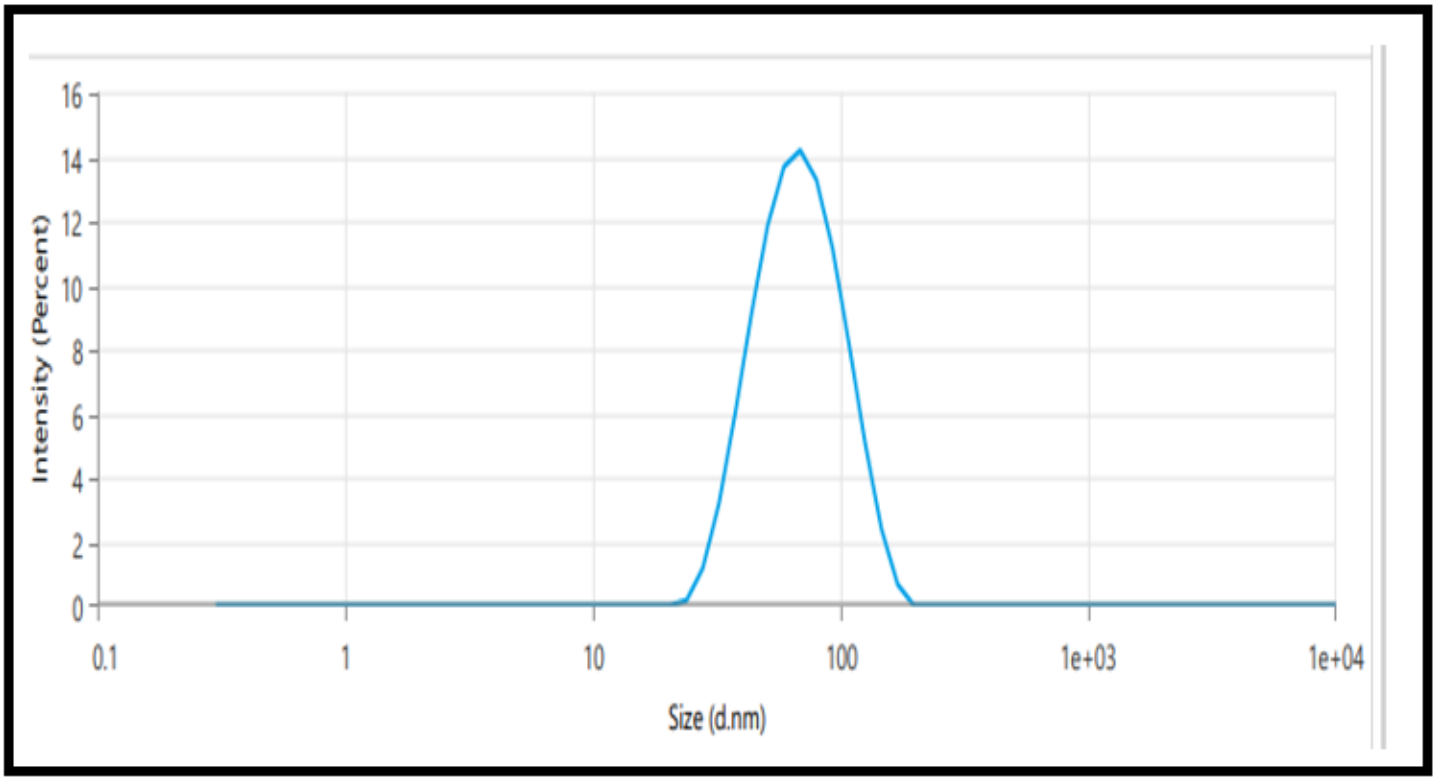

Figure 7

PSA of biosynthesized AgNPs

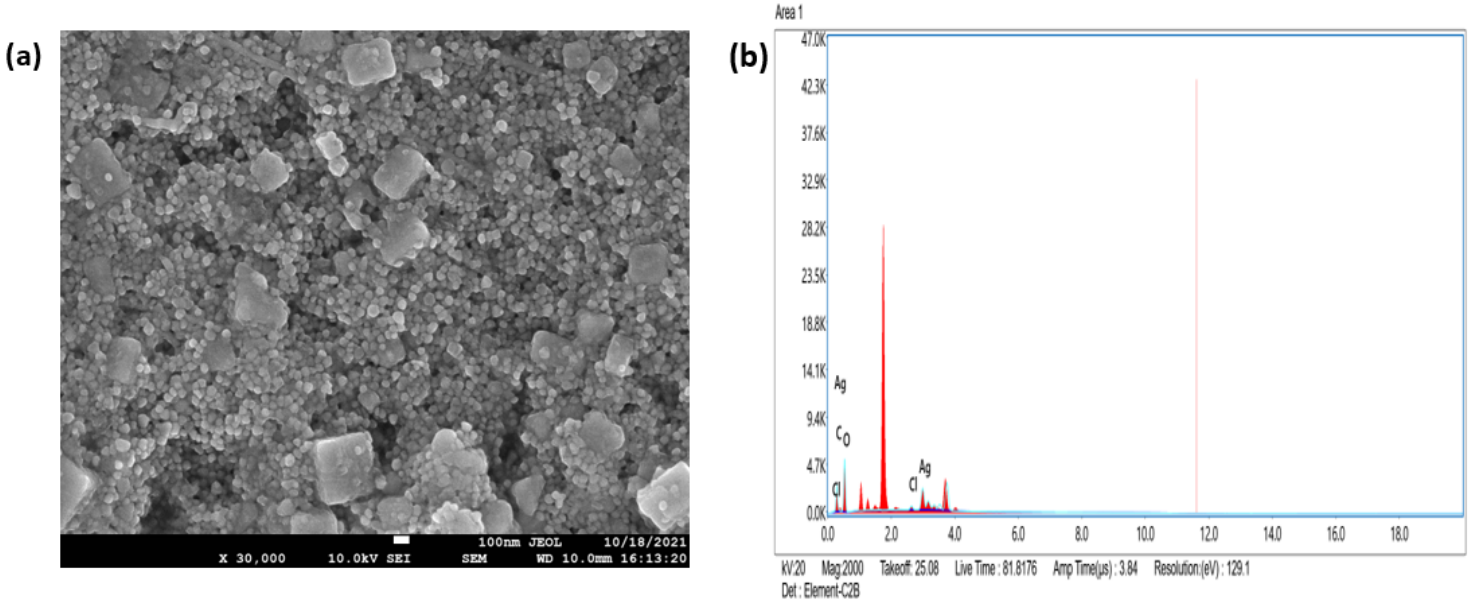

Figure 8

FESEM micrograph (a) 100 nm scale (b) elemental mapping of AgNPs

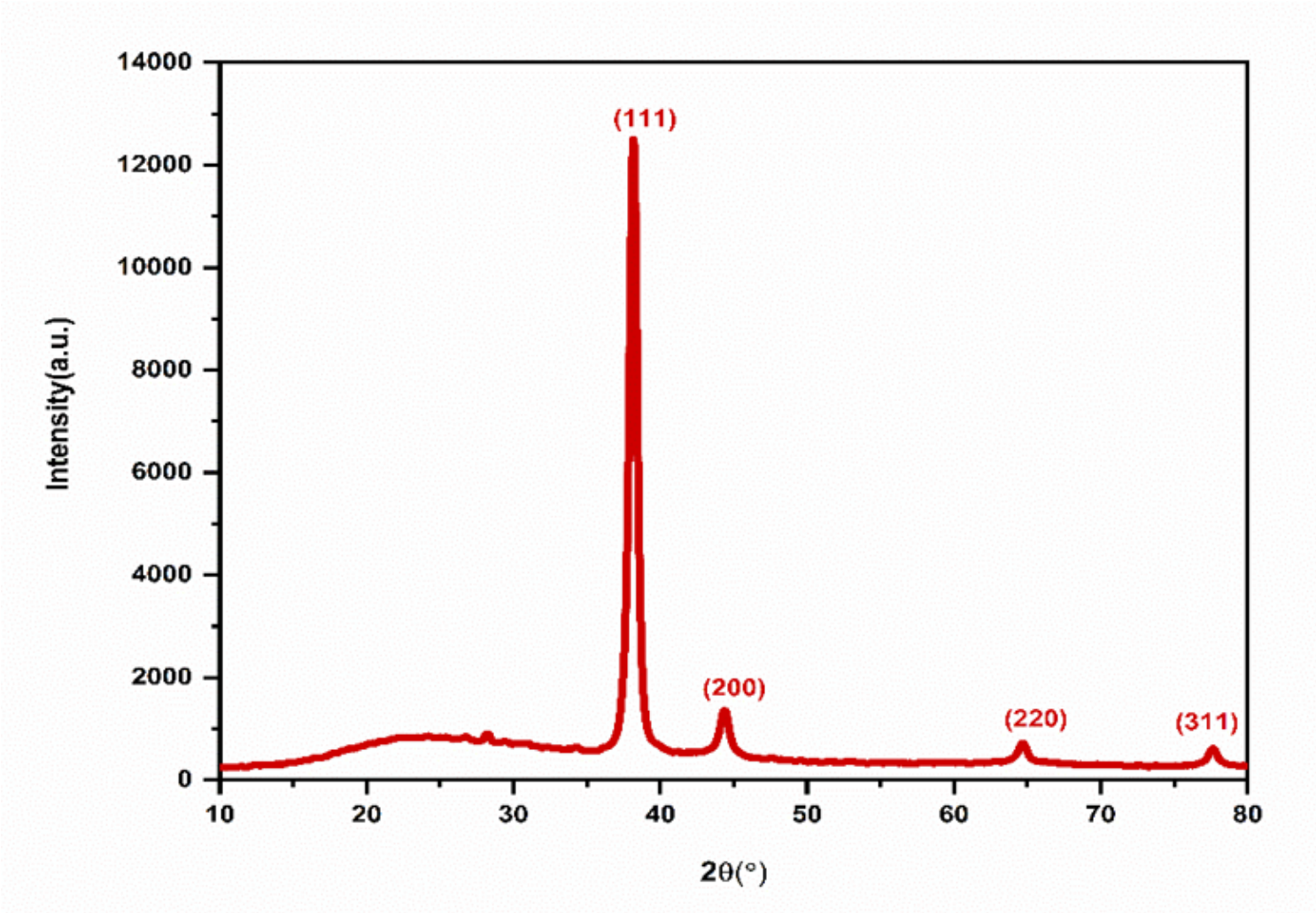

Figure 9

XRD of biosynthesized AgNPs

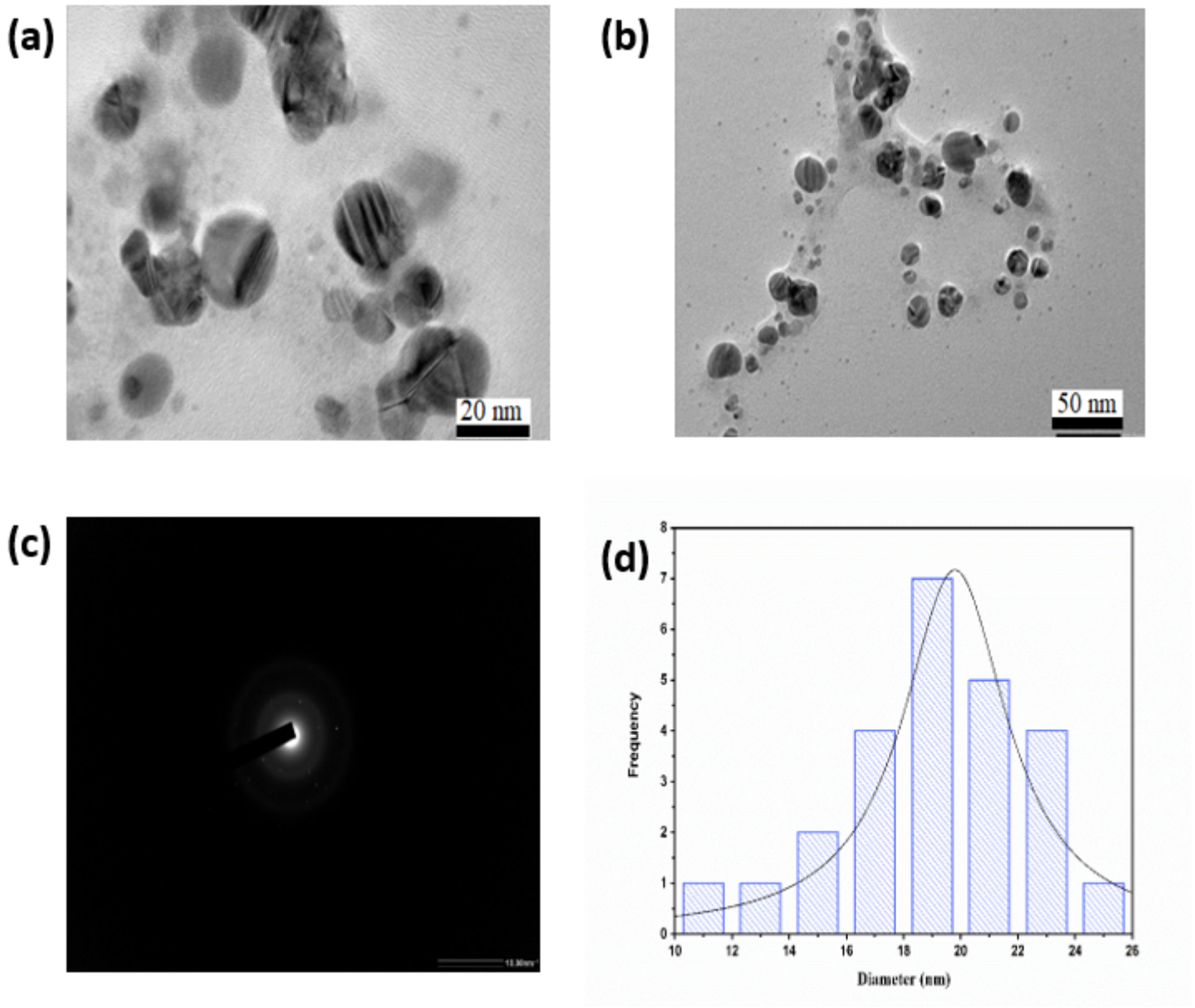

Figure 10

Images of HR-TEM showing the presence of AgNPs recorded at (a) 20nm (b) 50nm magnification levels (c) SAED pattern (d) histogram showing distribution of size of AgNPs

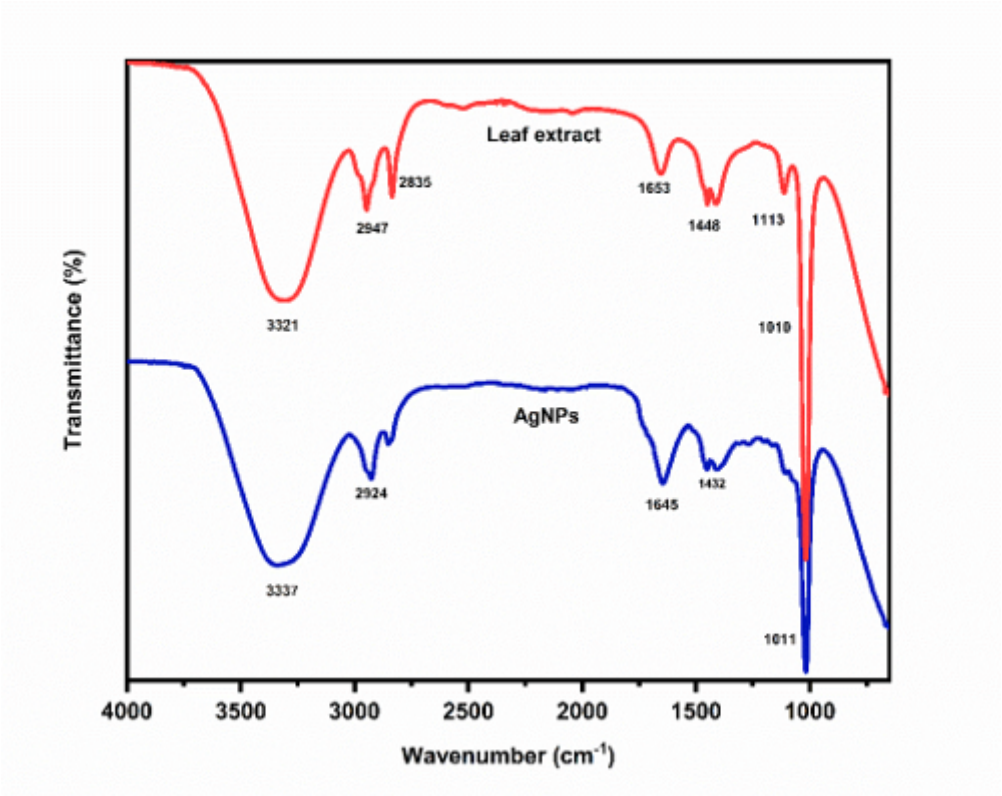

Figure 11

Comparative FT-IR spectra of leaves extract and their biosynthesized AgNPs

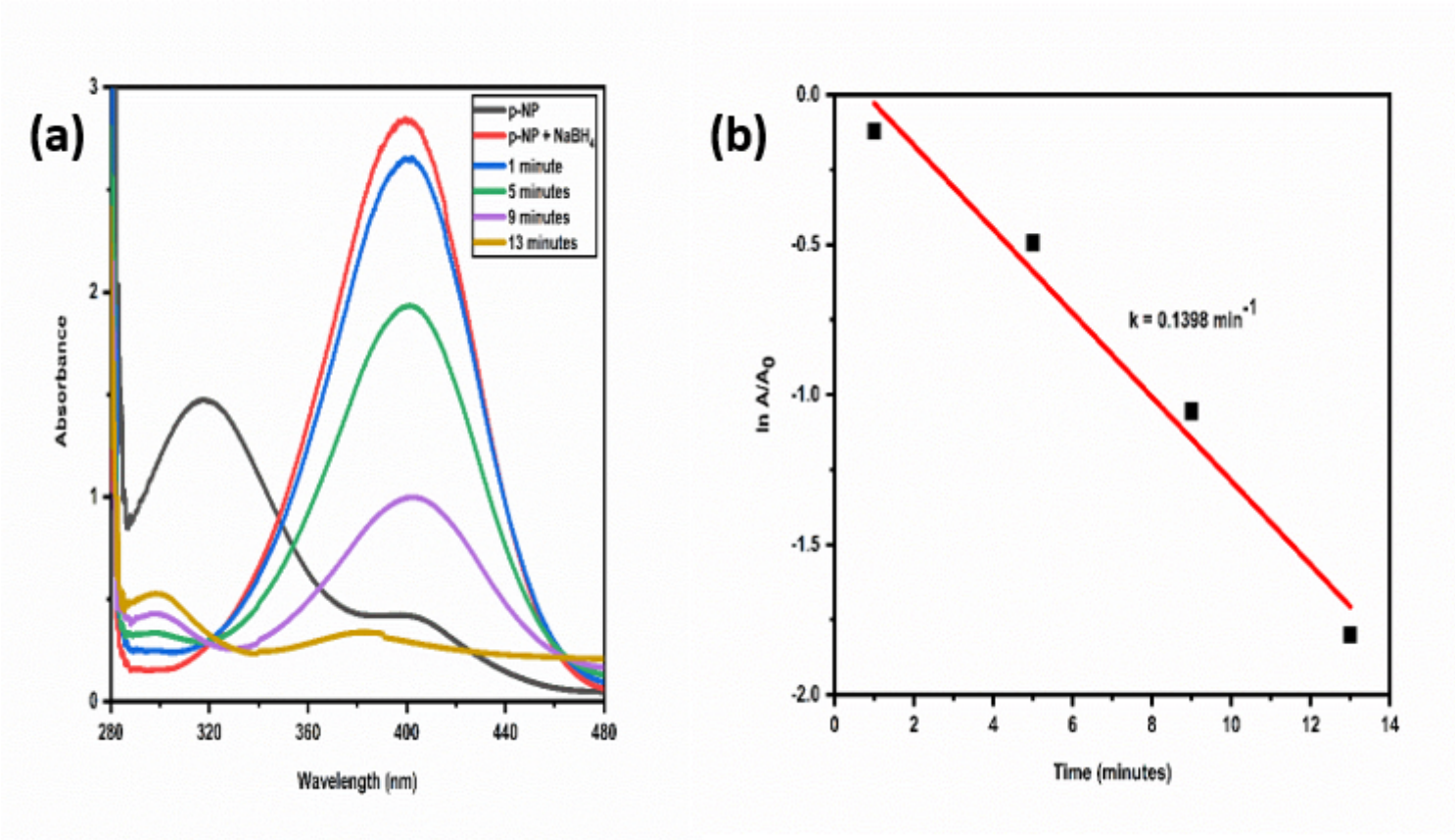

Figure 12

(a) Time dependent UV-vis spectra for the reduction of p- nitrophenol (p-NP) by $NaBH_4$ catalyzed using AgNPs (b) plot of ln[*A*] vs time for the reduction of p-NP using AgNPs

Supplementary Files

This is a list of supplementary files associated with this preprint. Click to download.

- Graphicalabstract.jpg